JOTCS A
Journal of the Turkish Chemical Society
Section: A
Chemistry
TURKISH CHEMICAL SOCIETY

Methanolysis of Gmelina Seed Oil to Biodiesel with KNO_3 Activated MgO-ZnO Composite Catalyst

Hamza R. Sani and Umar I. Gaya*

Department of Pure and Industrial Chemistry, Bayero University,
700241 Kano, Kano State, Nigeria

Abstract: The present study juxtaposes for the first time the heterogeneous methanolysis of gmelina oil over KNO_3 activated MgO-ZnO with a NaOH base methanolysis for biodiesel production. The conditions for biodiesel production such as temperature, reaction time, NaOH (or KNO_3 dose) and methanol-gmelina oil ratio were optimised. The 4%w/w KNO_3 activated MgO-ZnO afforded high biodiesel yield (71.5%) at 65 °C, predominantly consisting of C13-C25 cuts of linear fatty acid methyl esters (FAME). This heterogeneous catalyst was characterised using X-ray diffraction (XRD), energy dispersive X-ray (EDX) analyser, scanning electron microscopy (SEM) and Fourier transform infrared spectroscopy (FTIR). Gas-chromatography-mass spectrometry (GC-MS) revealed the selectivity to petroselinic acid methyl ester. The fuel properties of the biodiesel and its blends were consistent with standards. Relatively, the NaOH process yielded higher biodiesel (96.8%) at 60°C, 90 min, 1.2% NaOH and 9:1 methanol-oil ratio.

Keywords: Transesterification, methyl esters, composite, gmelina.

Submitted: December 03, 2018. **Accepted:** .July 30, 2019

Cite this: Sani H, Gaya U. Methanolysis of Gmelina Seed Oil to Biodiesel with KNO3 Activated MgO-ZnO Composite Catalyst. JOTCSA. 2019;6(3):335–48.

DOI: https://doi.org/10.18596/jotcsa.491458.

*Corresponding author. E-mail: uigaya.chm@buk.edu.ng. Tel: +2348039169418. Fax: +234-64-665-904.

INTRODUCTION

Concerns on the hike, non-renewability, unfriendliness, and non-biodegradable nature of crude oil products have jointly necessitated an intensive search for alternative fuels (1-3). By far, numerous approaches and technologies such as supercritical method (4), pyrolysis (5), emulsification (6) and transesterification (7) have been engaged in sustainable biodiesel production from fat- or oil-based triglycerides. Among these technologies, transesterification is at the forefront due to its greenness, cost-effectiveness, and convenient properties of triglyceride feed. Basically, transesterification involves the reaction of lipids with short-chain alcohols such as methanol (in a process called methanolysis) or ethanol (by ethanolysis), to yield long-chain fatty acid methyl esters (known popularly as biodiesel), and glycerol as co-product (8). Even though alkaline methanolysis is known to achieve high biodiesel yield in shorter process time, drawbacks such as catalyst recovery and severe corrosion necessitate the need to search for alternative materials such as heterogeneous catalysts and biocatalysts (9-12).

There has been considerable motivation to invest in heterogeneous biodiesel synthesis with emphasis on cost-effectiveness, biodiesel yield, process efficiency, the viability of the fatty acid feedstock and quality of the biodiesel produced (13-16). The high activity of co-precipitation-derived CaO-ZnO mixed oxides with or without doses of K_2CO_3 have proved effective for the methanolysis of sunflower oil (15,16). In the present study, we investigate the efficiency of KNO_3 activated, co-precipitation derived MgO-ZnO for the synthesis of biodiesel from gmelina oil. Because the industrial process of biodiesel synthesis exploits homogeneous alkaline catalysts, NaOH methanolysis was also studied. Nowadays, edible oils are considered unviable feedstocks and are marginally utilised in biodiesel

synthesis as opposed to vegetable and animal oils. The choice of gmelina oil for this study is therefore governed by the fact that it is non-edible and the source plant *Gmelina arborea* Linn. Roxb., is widely available in the wild of tropical countries (17).

MATERIALS AND METHODS

Seed samples and chemicals

The seeds of *Gmelina arborea* were collected from Bayero University Old Campus, Kano, in March, 2015. Methanol (99.8%, Sigma-Aldrich), $Zn(NO_3)_2.4H_2O$ (98%, BDH), $Mg(NO_3)_2.4H_2O$ (99%, BDH), KNO_3 (99%, BDH), NH_4OH (Sigma Aldrich, 36%), n-hexane (98%, Sigma Aldrich) were used as received from the manufacturers. Petrodiesel standard was obtained from Kaduna Refinery and Petrochemical Company (KRPC), a subsidiary of Nigeria National Petroleum Corporation (NNPC). De-ionised water was used in all preparations.

Oil extraction and pre-treatment

Gmelina oil was extracted from the *Gmelina arborea* seeds in the same manner described by Kansedo and Lee (18). Seeds were cleaned and dried in an oven at 100 ^oC overnight. The dry seeds were ground to fine particles using a mortar and pestle and then re-dried to remove moisture. The oil was extracted with n-hexane using soxhlet apparatus, operated at 70 ^oC for 4 h. Pre-treatment steps followed to remove free fatty acids from the oil were those of Šánek *et al*. (19). Exactly 40.7 g of the extracted oil was mixed thoroughly with 43.7 mL of methanol and 8.4 mL of 25% methanolic solution of tetramethylammonium hydroxide. The resultant mixture was shaken for 10 min and allowed to separate overnight in separating funnel and the phases so obtained were subsequently withdrawn and analysed.

Preparation of heterogeneous catalyst

The solid catalysts used in this work were prepared by co-precipitation followed by impregnation. The method of Istadi *et al.* (13) was applied, but substituting calcium for magnesium precursor. A solution of $Zn(NO_3)_2.4H_2O$ (2 mol/L) was co-precipitated with solution of $Mg(NO_3)_2.4H_2O$ (2 mol/L) in presence of NH_4OH. The gel formed was collected, washed with deionised water, and then dried in the oven overnight at 110 ^oC. The dry solid was calcined at 600 ^oC for 3 h in a muffle furnace to obtained MgO-ZnO composite. This material was then impregnated with appropriate amounts of KNO_3 and dried in an oven at 110 ^oC overnight to produce 1 to 6%w/w. The resulting solid catalysts were calcined in the furnace at 600 ^oC for 3 h.

Heterogeneous methanolysis

The production of biodiesel by using the KNO_3 activated MgO-ZnO catalysts was performed in a two-necked 500 mL glass reactor, and fitted with a condenser and thermometer. The catalyst amount was fixed at 0.8 g, but the impregnation solution was varied from 1 to 6%w/w. Prior to methanolysis, the catalyst was first activated in methanol at 40 ^oC with constant stirring for 40 min. After activation of the catalyst, 40 g of oil (heated at 100 ^oC for 30 min prior to the reaction) was added to the batch reactor. The system was agitated using a magnetic stirrer. In order to separate the catalyst, the resulting mixture was filtered through a Whatman filter paper (125 mm diameter, 2.5 µm pore size). The filtrate was allowed to stand for 24 h in separating funnel. Subsequently, the glycerol resident at the bottom was separated from the biodiesel. The percentage of biodiesel yield was calculated using the following equation:

$$\text{Biodiesel yield } (\%) = \frac{\text{weight of biodiesel produced}}{\text{weight of oil used}} \times 100 \quad (1)$$

Homogeneous methanolysis

In order to compare the rate of the heterogeneous methanolysis with the conventional NaOH base methanolysis, biodiesel was produced using a previously described method (20). Exactly 40 g of oil was measured and poured into 500 mL round bottom flask. The catalyst was weighed and 20 mL methanol was added to it in a conical flask and stirred until the pellet dissolves, to form sodium methoxide solution. The solution was poured into the oil; the resultant mixture was refluxed at 50 to 70 ^oC for 90 min, in the presence of desired methanol to oil molar ratio and a known amount of NaOH. Agitation speed was 600 rpm. After completion of the reaction, the mixture was transferred into a separating funnel and allowed to stand overnight to allow for proper settling of the glycerol.

In order to remove residual by-products such as soap, residual methanol and glycerol, the biodiesel produced was purified by several washing cycles, using de-ionized water. The biodiesel was diluted (30%), stirred for 2 min and transferred to a clean separating funnel and allowed to stand for 5 h. The top layer was pure biodiesel. The impure bottom layer was re-extracted repeatedly until no appearance of by-products. The resulting biodiesel was then allowed to form pure biodiesel (B100) by standing for 24 h. Biodiesel blends, B20 and B50, were prepared by mixing petroleum diesel and pure biodiesel in a ratio of 80:20 and 50:50.

Gmelina oil and biodiesel characterisation

Free fatty acids (FFA) content and a saponification value of the gmelina oil were determined using the titrimetric methods described by the American Oil Chemists Society (AOAC) (21, 22). Fuel properties of the gmelina oil, biodiesel and petrodiesel such as kinematic viscosity, flash point, cloud point and specific gravity were determined using the methods of American Society for Testing and Materials (ASTM) (23). The composition analysis of the biodiesel was

performed with the aid of gas chromatography-mass spectroscopy (GC-MS) using a Shimadzu QP2010 Plus GCMS. The injector of the GC was kept at 200 ^{o}C. Injection mode was split by a ratio of 20. The column was VF-5, held at 60 ^{o}C for 2 min and ramped at the rate of 10 ^{o}C/min to 280 ^{o}C for 7 min.

Effect of reaction variables

The operation parameters (methanol to oil molar ratio, KNO_3 loading levels, reaction time and temperature) for the heterogeneous system were varied from 3:1 to 18:1, 1 to 6%w/w, 2 to 7 h, 45 to 65 ^{o}C by the classical one factor at a time method at fixed agitation velocity (600 rpm), catalyst amount (0.8 g) and initial gmelina oil mass (40 g). All parameters were optimised. The potential of reuse of the solid catalyst was investigated at the optimised conditions using the recovery method. On the other hand, the homogeneous process was investigated using 3.1 to 9:1 methanol to oil molar ratios, 0.4 to 2.0% NaOH for 30 to 90 min reaction times at 45 to 70 ^{o}C.

Characterization of the solid catalyst

The solid catalyst with an outstanding performance was characterised. X-ray diffraction (XRD) analysis was performed on a Philips X'Pert Pro diffractometer, using Cu-Kα source (λ=1.56877 Å). The diffractometer was run at 30 kV and 30 mA, over a 2θ range of 10^{o} to 120^{o}. Scanning electron microscopy was carried out on Leica Stereoscan-440 SEM hyphenated with Phoenix energy dispersive X-ray analyser. Crystallite size was estimated using the Debye-Scherer formula:

$$D = \frac{k\lambda}{\beta\cos\theta} \qquad (2)$$

where D is the crystalline diameter; k is the crystallographic constant (0.9, for spherical crystals), λ is the wavelength of CuKα radiation, 0.156877 nm; β is the full width of half maximum (FWHM) while θ is the diffraction angle. As crystallite sizes depend mainly on diffraction angles, the average crystallite size of the catalyst was calculated using equation (3).

$$\text{Average crystallite size} = \frac{\sum(\text{crystallite size})}{\text{Number of peaks}} \qquad (3)$$

Elemental measurements were carried out on Leica Stereoscan-440 scanning electron microscope instrument interfaced with Phoenix Energy-dispersive X-ray spectrometer. The instrument was operated using Pd X-ray tube at 25 kV and 1.2 mA. Fourier transform infrared spectroscopy was performed on an Agilent Cary 630 diamond attenuated total reflectance Fourier transform infrared spectrometer (ATR-FTIR), within a spectral range of 1000-650 cm^{-1}.

RESULTS AND DISCUSSION

Catalyst characterization

The crystalline structure of 4% w/w KNO_3 activated MgO-ZnO, the best performing composite, was characterised using XRD plot (Figure 1). From the figure, the XRD peaks of ZnO are clearly seen at 2θ angle of 31.8^{o}, 34.48^{o}, 36.3^{o}, 47.6^{o}, 56.6^{o}, 62.9^{o}, 66.47^{o}, 69.1^{o}, 71.8^{o}, 76.8^{o}, 80.7^{o} (JCPDS card 36-1451). The diffractogram also clearly reveals peaks of MgO at 2θ angle of 42.9^{o}, 53.76^{o}, 62.2^{o}, 73.7^{o}, 78.6^{o}, 83.7^{o}, 86.1^{o} (JCPDS file 01-072-0447). It also shows reflection peaks consistent with that of K—O (JCPDS file 77-2176) with 2θ angles of 23.08^{o}, 26.7^{o}, 28.96^{o}, 40.7^{o}, 82.78^{o}, 90.1^{o}, 91.3^{o}, 109.76^{o}. The average crystallite size of the catalyst was calculated using Debye-Scherer equation to be 66.45 nm.

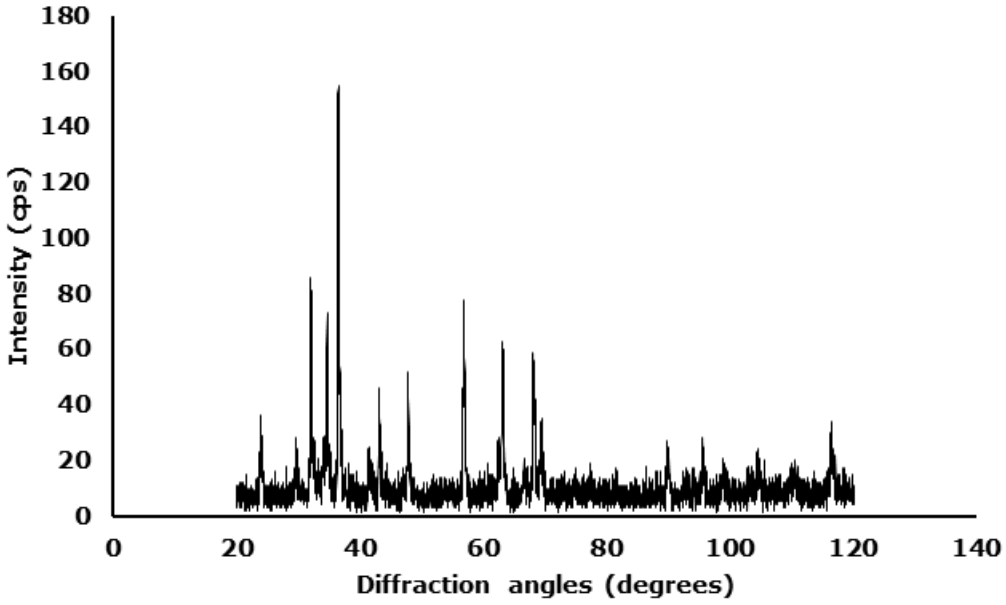

Figure 1. The X-ray diffractogram of 4%w/w KNO_3 activated MgO-ZnO.

The external morphology of the synthesised catalyst is displayed in Figure 2. The SEM image shows lumps of organised grains. Section analysis informs of the dimension of the grains to be in the order of hundreds to a thousand plus nanometer.

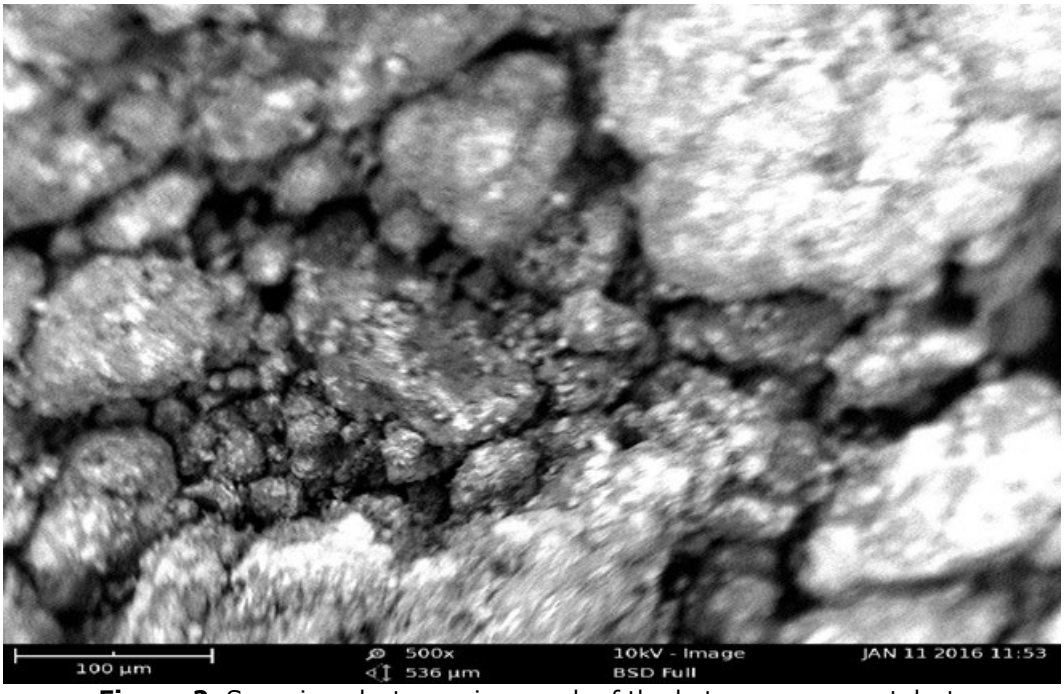

Figure 2. Scanning electron micrograph of the heterogeneous catalyst.

The elemental composition of the 4% w/w KNO_3 activated MgO-ZnO catalyst is presented in Table 1. The ratios of the EDX peak concentrations in the table revealed atomic ratios which confirm the formula of 4% w/w KNO_3 activated MgO-ZnO catalyst to be the non-stoichiometric oxide $K_{4.08}N_{0.73}Mg_{0.54}$-$ZnO_{2.38}$. The ATR-FTIR spectrum of the prepared catalyst revealed the sharp peak between at 527 cm^{-1} characteristics of stretching mode of Zn-O bond (24). The incorporation of Mg^{2+} into the ZnO crystal structure is corroborated by the intense Mg-O peak at 474 cm^{-1} (25). The formation of K-O bond was confirmed by the peak at 491 cm^{-1}.

Table 1. Energy dispersive X-ray data of the composite.

Element	Weight percentage (%)	Relative ratios
K	48.1	4.08
O	25.1	2.38
Zn	11.8	1.00
Mg	6.4	0.54
N	8.6	0.73

Optimisation of reaction conditions

Primarily, the methanolysis of oil to biodiesel is a stoichiometric reaction involving 1 mole of triglyceride with 3 moles of methanol to yield methyl esters and glycerol. However, because the methanolysis of triglycerides is a reversible reaction excess methyl alcohol is required to favour the rate of reaction that forms the biodiesel. The yield-methanol profiles for both the heterogeneous catalyst and the NaOH mediated counterpart are shown in Figure 3. The figure shows a general increase in the yield of the methyl ester with increasing methanol-oil ratio from 3:1 up to 12:1 for the solid catalyst (and 9.1 for the NaOH catalysed process). This may be attributed to the equilibrium shift in the direction of methyl ester. Excess amounts of methyl alcohol do not improve the biodiesel yield as indicated by the levelling off of both curves in Figure 3. The decline in yield may be as a result of the dissolution of glycerol in the excess methyl alcohol which hinders the interaction of the reactants with the catalyst. From the figure, the methanol to oil molar ratio of 12:1, with a yield of 72.85%, is considered optimum for the heterogeneous process while 9:1 is optimum for the homogeneous process. Feyzi and Shahbazi (3) achieved a higher yield (96.1%) with 6 wt% Al-Sr/ZSM-5 catalyst at a methanol-oil molar ratio of 12:1.

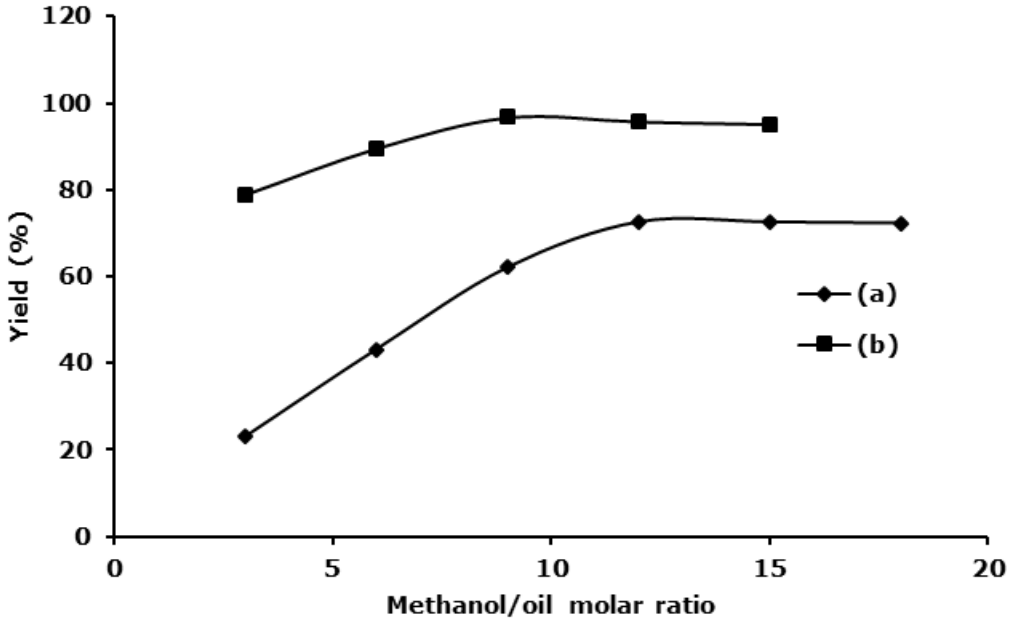

Figure 3. Effect of methanol to oil molar ratio on biodiesel yield in presence of (a) 1% NaOH catalyst. Temperature = 65 ^{o}C, agitation velocity = 600 rpm, initial mass of oil = 40 g, reaction time = 90 min. (b) 4% w/w KNO_3 activated MgO-ZnO catalyst. Mass of gmelina oil = 40 g, reaction temperature = 60 ^{o}C, reaction time 4h, catalyst loading = 0.8 g, stirring speed = 600 rpm.

The influence of KNO_3 promoter (1 to 6% w/w) in the MgO-ZnO catalysts was investigated at the predetermined optimum methanol-oil ratio. The methyl ester yield increased proportionally with the addition of 1 to 4% w/w KNO_3, with the highest yield (72.85%) corresponding to the limiting catalyst dose (4% w/w) (Figure 4). Therefore, KNO_3 loading of 4% w/w is optimum for the heterogeneous methanolysis. A yield of 90% was earlier reported when K-La was used as a promoter of ZSM-5 zeolite for the methanolysis of soybean oil (26).

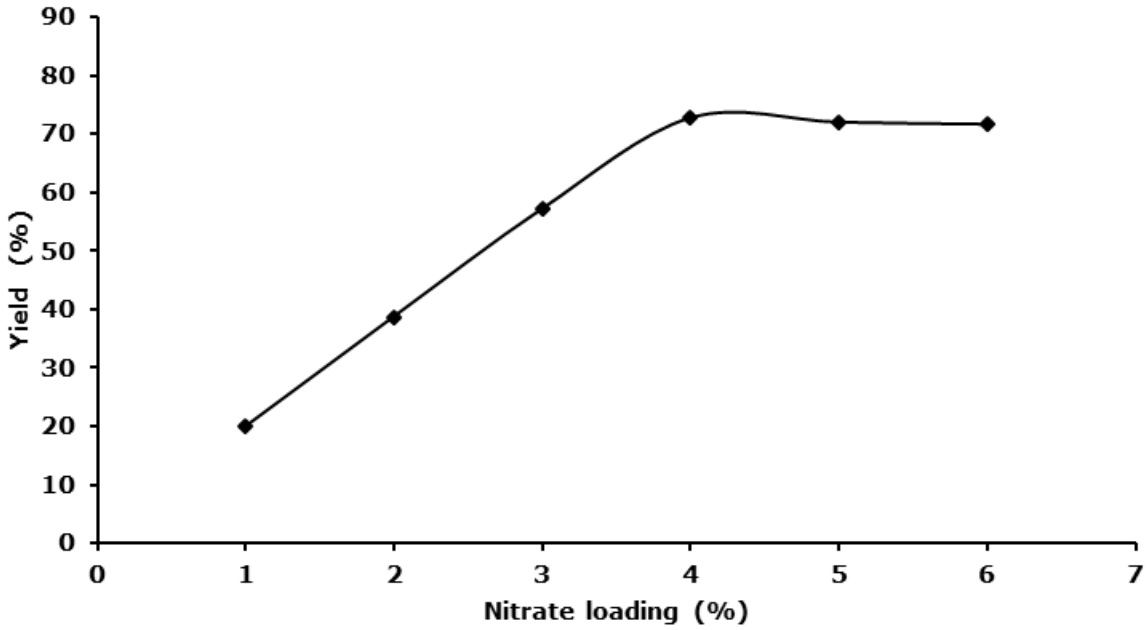

Figure 4. Effect of KNO_3 levels on the performance of the MgO-ZnO catalyst for the biodiesel synthesis. Mass of gmelina oil = 40 g, Mass of MgO-ZnO (0.8 g), temperature = 60 °C, reaction time = 4 h, methanol to oil molar ratio = 12:1, stirring speed = 600 rpm.

In the homogeneous methanolysis, the influence of NaOH (0.4 to 2%) was investigated at the optimum methanol-oil ratio. Increasing presence of NaOH from 0.4 to 1.2% enhanced the yield, with maximum yield (98.1%) corresponding to 1.2% NaOH (Figure 5). The decline in biodiesel yield above 1.2% NaOH (Figure 5) can be attributed to a high concentration of by-products. Therefore, a base catalyst loading of 1.2% was applied in the homogeneous methanolysis.

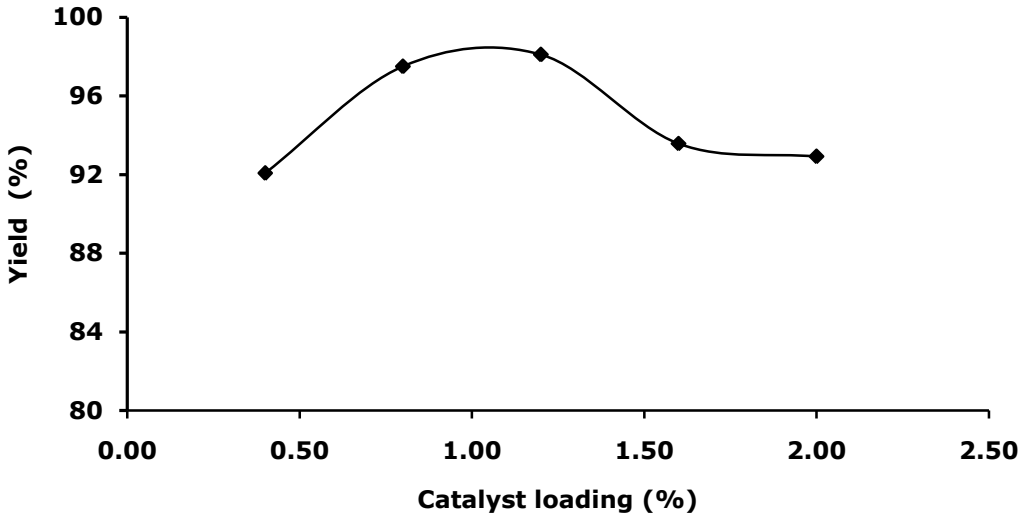

Figure 5. Effect of NaOH on biodiesel yield. Reaction time = 90 min, methanol-oil molar ratio = 9:1, temperature = 65 °C, stirring speed = 600 rpm, mass of gmelina oil = 40 g.

Reaction temperature is one of the most important parameters that influence biodiesel yield. The reaction temperature was investigated in a range of 45 to 70 °C for the solid catalyst and 45 to 65 °C for the NaOH mediated process (Figure 6). Biodiesel yield was enhanced until 65 (or 60) °C for the heterogeneous (or homogeneous) process. This can be linked to corresponding enhancement of miscibility and mass transfer. Above this temperature biodiesel yield does not increase, likely due to the volatilisation of methanol and its decreasing polarity, hence the sodium methoxide population.

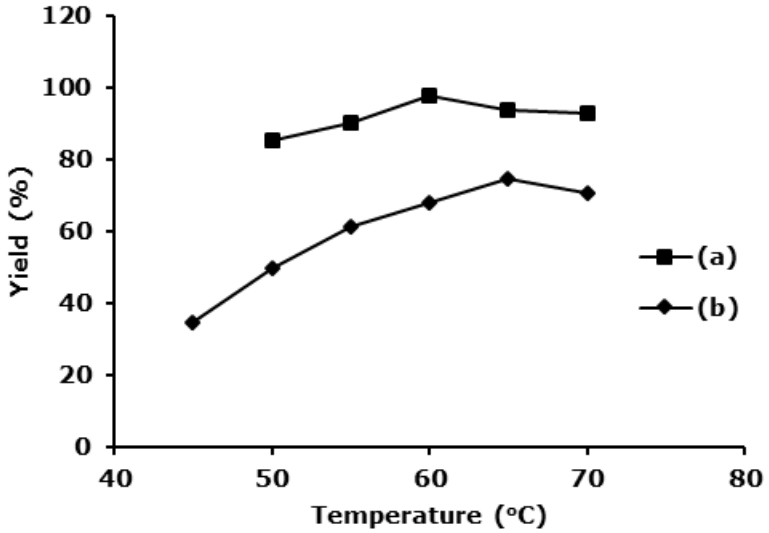

Figure 6. Effect of reaction temperature on biodiesel yield in presence of (a) 0.8 g of 4% w/w KNO_3/MgO-ZnO. Mass of gmelina oil = 40 g, methanol-oil molar ratio = 12:1, reaction time = 7 h, stirring speed = 600 rpm (b) 1.2% NaOH. Reaction conditions: methanol-oil molar ratio = 9:1, reaction time = 90 min, stirring speed = 600 rpm.

The influence of reaction time was studied between 2 and 7 h, at optimum temperature (60 °C), catalyst loading (0.8 g of 4 wt% KNO_3/MgO-ZnO), methanol-oil molar ratio (12:1) and at a constant stirring speed (600 rpm). As shown in Figure 7, the biodiesel yield increases progressively with increase in reaction time and reached its maximum (71.5%) at 7 h. This catalyst was chosen as optimal for the biodiesel synthesis. The optimal catalyst is not very active (yield <90%) (15). However, it is not uncommon with yields of biodiesel yield to be lower than this threshold, especially with heterogeneous catalysts. A yield of 87.7% was obtained with ZSM-5 supported Ba-Sr nanocatalyst at optimum operating conditions (27).

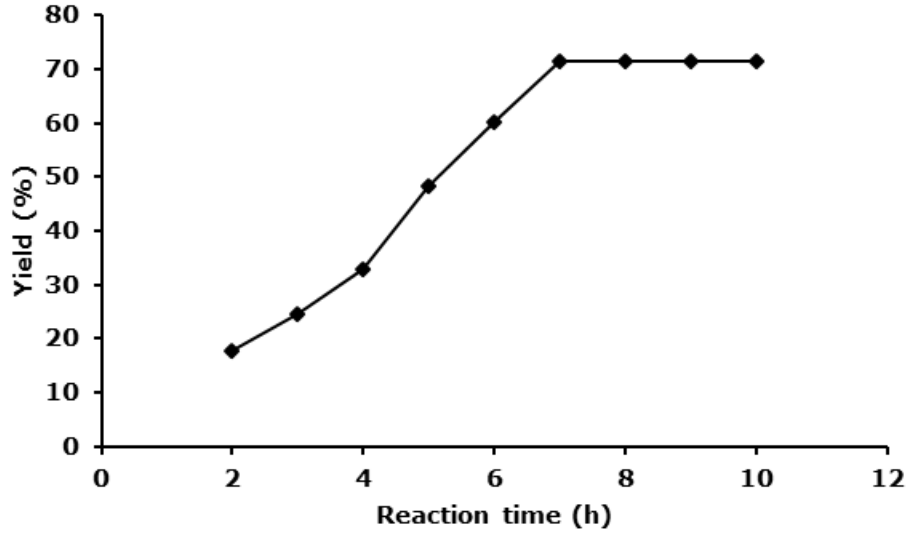

Figure 7. Effect of reaction time on biodiesel production over KNO_3 activated MgO-ZnO.

The influence of reaction time in this NaOH mediated methanolysis was performed in a range of 30 to 90 min at constant temperature (60 °C), methanol-oil molar ratio (9:1), catalyst loading (1.2%), gmelina oil (40 g) and stirring speed (600 rpm). The results show an increase in biodiesel yield with an increase in reaction time up to 90 min with a maximum yield of 96.8% (Figure 8).

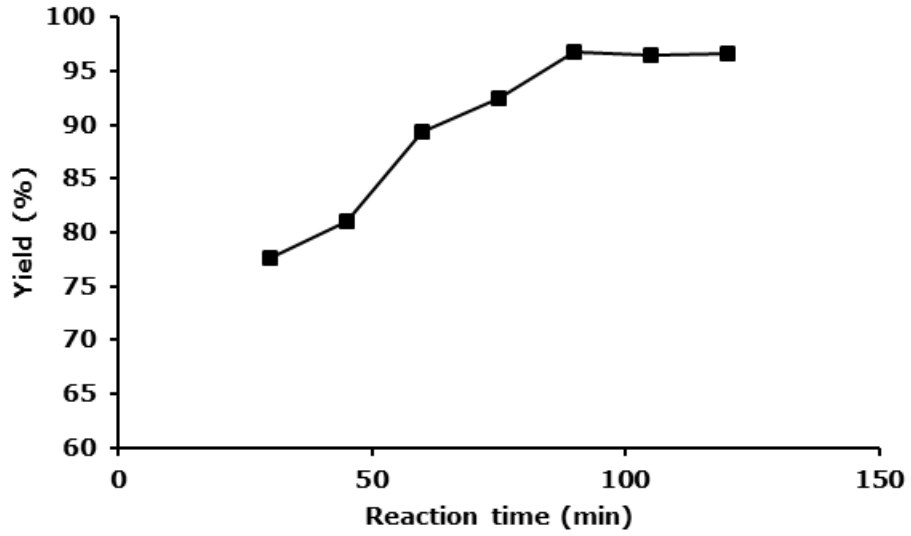

Figure 8. Effect of reaction time on biodiesel production using NaOH.

Oil characterisation

Prior to and after extraction of the gmelina oil, drying and pretreatment, acid value, free fatty acids and saponification values are given in Table 2. Gmelina oil was found to have high acid value (11.6 mg KOH/g) prior to pretreatment when compared to those from Karanja oil (5.06 mg KOH/g) (28). The saponification value of the oil declined by 4%, while the free fatty acid (FFA) value and the acid value was lowered by 82%. The FFA value obtained after pretreatment (1.056%) implies a low tendency to undergo saponification.

Table 2. Properties of gmelina seed oil.

Property	Before pretreatment	After pretreatment
Acid value (mg KOH/g oil)	11.64	2.10
Free fatty acids (%)	5.85	1.06
Saponification value (mg KOH/g oil)	194	186

The fuel properties exhibited by gmelina oil, biodiesel (B100), the blends B20 and B50 and those of petrodiesel were determined (Table 3). Due to exceedingly high fuel properties such as cloud point (6 ^{o}C), flash point (126 ^{o}C), kinematic viscosity (11.91 mm^2/s) and specific gravity, the gmelina oil must be upgraded or converted to another form prior to application as fuel. A comparison with petrodiesel shows the unsuitability of the gmelina oil for use as fuel. Upon methanolysis however, the biodiesel product and its blends exhibit properties consistent with those of ASTM standard. Specifically, the specific gravity (0.86) is more or less that of typical biodiesel (0.88) (29). The viscosity of the gmelina oil was reduced to 3.66 mm^2/s, a value that is lower than that of Moringa oleifera methyl esters (4.83 mm^2/s) (30). Similarly, the specific gravity of gmelina oil is reduced down to acceptable values, by conversion to biodiesel blends B100, B50 and B20. The cloud point of the oil and B100 (-5 ^{o}C) nears that of typical cottonseed oil (-4 ^{o}C) (31). The B100 Furthermore, the biodiesel and its blends (Table 3) are inherently "sweet" (with S content << 0.5%) which is usual with biomass oils and consistent with green emissions. The sulphur content of B100 and gmelina oil is even lower than that of petrodiesel. The cetane number for B100 was determined to be 51.7 which complies with ASTM (23). The value measured in this study is slightly higher than that reported for castor biodiesel (48.9) (32).

Table 3. Fuel properties of gmelina oil, biodiesel and its blends with petrodiesel.

Fuel properties	Unit	Petrodiesel	Gmelina oil	B100	B50	B20	ASTM (23)
Kinematic viscosity @40°C	cSt	2.60	11.91	3.66	3.10	2.91	1.9-6.0
Sp. Gravity @27°C	kg/L	0.846	0.90	0.863	0.860	0.846	0.860-0.900
Flash point	°C	49	126	106	80	56	100-170
Combustion point	°C	59	125	96	91	65	-
Cloud point	°C	-5	6	2	-2	-5	-6 to 12
Sulphur content	%	0.167	0.012	0.0220	0.0929	0.100	-
Cetane number	°C	-	ND[a]	51.7	49.5	48.6	48-65

[a]Not determined

Methanolysis products

The products of methanolysis were detected by GC-MS. The chromatographic peaks (Fig. 9) were interpreted using NIST107.LIB GC library.

There are fourteen peaks on the chromatogram, corresponding to different fatty acid methyl esters. These fatty acid methyl esters and their retention property are displayed in Table 4. Majority of the compounds have a base peak at m/z = 74 indicating a common fragment $[CH_2{=}CHCH_2CH_2]^+$. The compound petroselinic acid methyl ester (or 6-octadecanoic acid methyl ester) eluted at 20 min retention time, has the broadest and most intense peak and accounts for about 62% of the fatty acid methyl esters yield of the methanolysis process. It was earlier noted from Table 4 that the cloud point of B100 is higher than petrodiesel, though within the acceptable range. This can be explained based on the waxing of the major product and other methyl esters which emerged at higher retention times (Table 4) at extremely low temperatures.

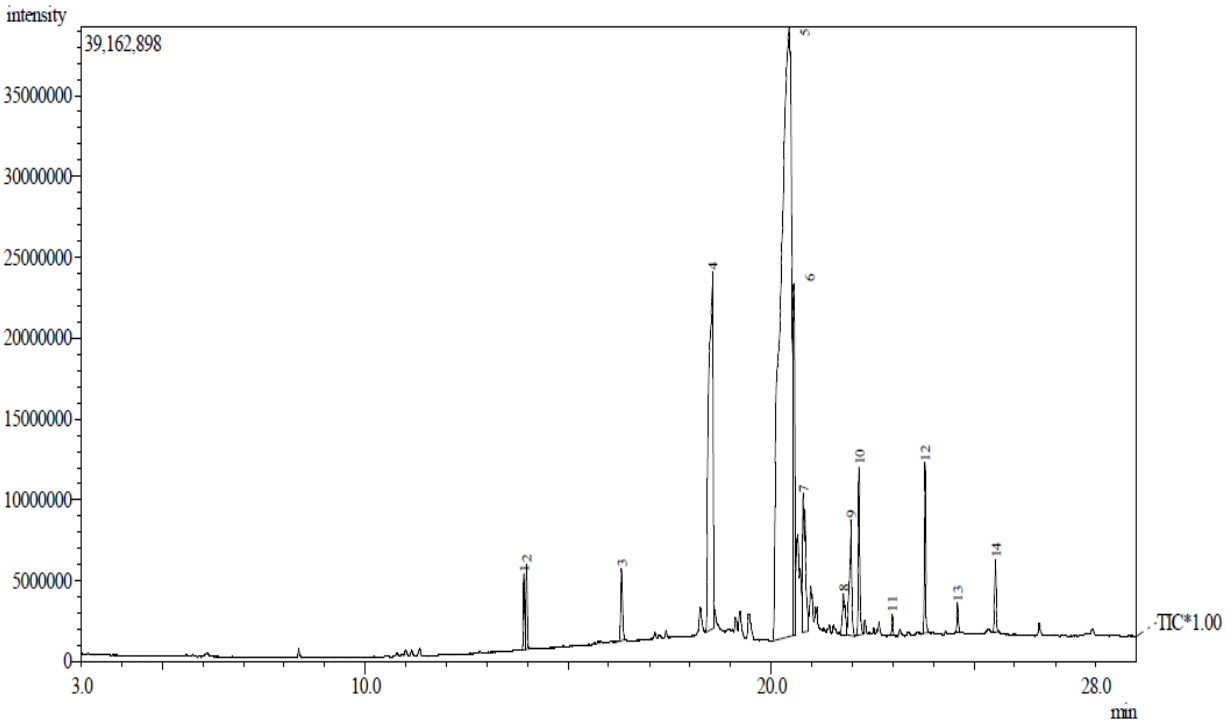

Figure 9. Elution peaks of fatty acid methyl esters with petroselinic acid methyl ester dominating the chromatogram.

Table 4. Chemical and common names of the fatty acid methyl ester (FAME) of the as-prepared biodiesel.

Peak No.	Retention time (min)	Peak area (%)	Assignment of peaks	C atoms
1	13.908	0.94	Dodecanoic (capric) acid methyl ester	C_{13}
2	13.975	0.98	Tridecanoic acid methyl ester	C_{14}
3	16.317	1.21	Tetradecanoic (myristic) acid methyl ester	C_{15}
4	18.550	14.22	Hexadecanoic (or palmitic) acid methyl ester	C_{18}
5	20.442	62.22	6-octadecanoic (or petroselinic) acid methyl ester	C_{19}
6	20.567	6.37	Octadecanoic (or stearic) acid methyl ester	C_{19}
7	20.792	3.97	Linolelaidic (or 9,12-Octadecadienoic) acid methyl ester	C_{19}
8	21.783	1.18	5,8-octadecadienoic acid methyl ester	C_{19}
9	21.958	2.41	9-octadecanoic (or elaidic) acid methyl ester	C_{19}
10	22.167	2.39	Eicosanoic (arachidic) acid methyl ester	C_{21}
11	22.983	0.26	Heptacosanoic acid methyl ester	C_{22}
12	23.792	2.30	Docosanoic (or behenic) acid methyl ester	C_{23}
13	24.592	0.39	Tricosanoic acid methyl ester	C_{24}
14	25.525	1.17	Tetracosanoic (or lignoceric) acid methyl ester	C_{25}

Reusability of the KNO_3 activated composite

Recovery of the synthesized catalyst was evaluated using 12:1 methanol to oil molar ratio, 65 °C reaction temperature, and reaction time of 7 h. After each run, the spent catalyst was recovered, washed with petroleum ether to remove the adsorbed materials. This catalyst was then reactivated for reuse by calcination in a muffle furnace for 2 h at 400 °C. The results (Figure 10) showed that the catalyst can be reused for five consecutive runs while maintaining considerable methanolytic activity (above 50%). The decrease in biodiesel yield from 72.5% in the first cycle to 56.8% after five cycles may be attributed to deactivation of the catalyst sites caused by the various chemical species undergoing competitive adsorption and desorption.

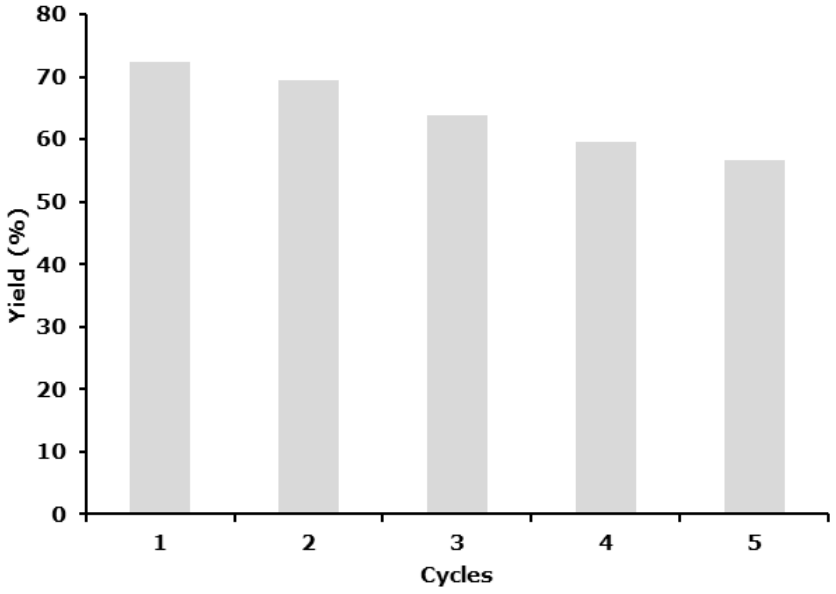

Figure 10. Effect of $K_{4.08}N_{0.73}Mg_{0.54}$-$ZnO_{2.38}$ recycling on biodiesel yield. Reaction conditions: Time = 7 h, temperature = 60 °C, catalyst loading = 0.8 g of 4% w/w KNO_3/MgO-ZnO, methanol-oil molar ratio = 12:1 and stirring speed = 600 rpm.

Transesterification kinetics

Generally, transesterification reactions proceed through three elementary steps comprising the conversion of triglyceride to diglyceride (the rate-limiting), diglyceride to monoglyceride and then finally monoglyceride to fatty acid methyl esters (FAME) and glycerol. The triglyceride conversion is traditionally first-order and can be used to evaluate the reaction rate constant (33). Basically, the logarithmic function of FAME is related to time by the equation:

$$\ln[FAME]_t - \ln[FAME]_0 = k't \quad (4)$$

Where $[FAME]_0$= initial concentration of fatty acid methyl ester at time t = 0 and $[FAME]_t$ is the concentration at time t. The plot of $\ln[FAME]_t$ against *t* (Figure 11) for the heterogeneous system gives a straight line with a correlation coefficient (R^2) of 0.986 indicating consistency with pseudo-first-order. The slope of the plot which equals to the rate constant (*k*) of the heterogeneous process is 4.8 x 10^{-3} min^{-1}. The corresponding rate constant for the NaOH base methanolysis was found to be 3.8 x 10^{-3} min^{-1}.

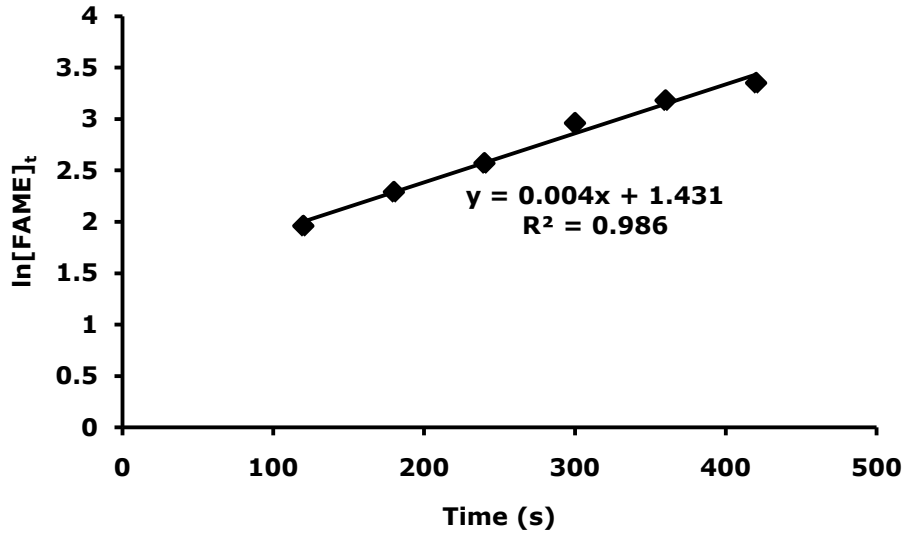

Figure 11. First-order kinetic plot of gmelina oil conversion over KNO_3 activated MgO-ZnO composite.

Activation parameters

Temperature dependence results permitted the estimation of energies of activation. The logarithmic function of the rate constant for the biodiesel production is related to activation energy by the Arrhenius equation (5).

$$lnk = lnA - \frac{Ea}{RT} \quad (5)$$

Where A is the Arrhenius factor (hr^{-1}), E_a is the activation energy (J/mol K), R is the molar gas constant (8.314 J /mol K) and T is the absolute temperature (K). Activation functions were obtained from the plot of lnk against *1/T* (Figure 12). The activation energy and the pre-exponential factor for the $K_{4.08}N_{0.73}Mg_{0.54}$-$ZnO_{2.38}$ mediated biodiesel synthesis are 68.92 kJ/mol and 9.698×10^7 min^{-1}, respectively, while the corresponding values for the NaOH-assisted process are 38.55 kJ/mol, 2.75×10^4 min^{-1}.

The Eyring equation (expressed as Equation (6)) permits the estimation of other energies of activation (ΔG^*, ΔH^*, ΔS^*).

$$\ln\left(\frac{k}{T}\right) = -\left(\frac{\Delta H}{RT}\right) - \left[\ln\left(\frac{k_b}{h}\right) + \frac{\Delta S}{R}\right] \quad (6)$$

Where k_b is the Boltzmann constant (1.38×10^{-23} J/K) and h is the Plank's constant (6.63×10^{-34} Js) while other quantities have their usual meaning. A plot of $\ln\left(\frac{k}{T}\right)$ against the inverse of temperature (*1/T*) at 338 K as in Figure 13 gives a slope equal to $-\frac{\Delta H}{R}$ while the intercept provides $\frac{\Delta S}{R}$.

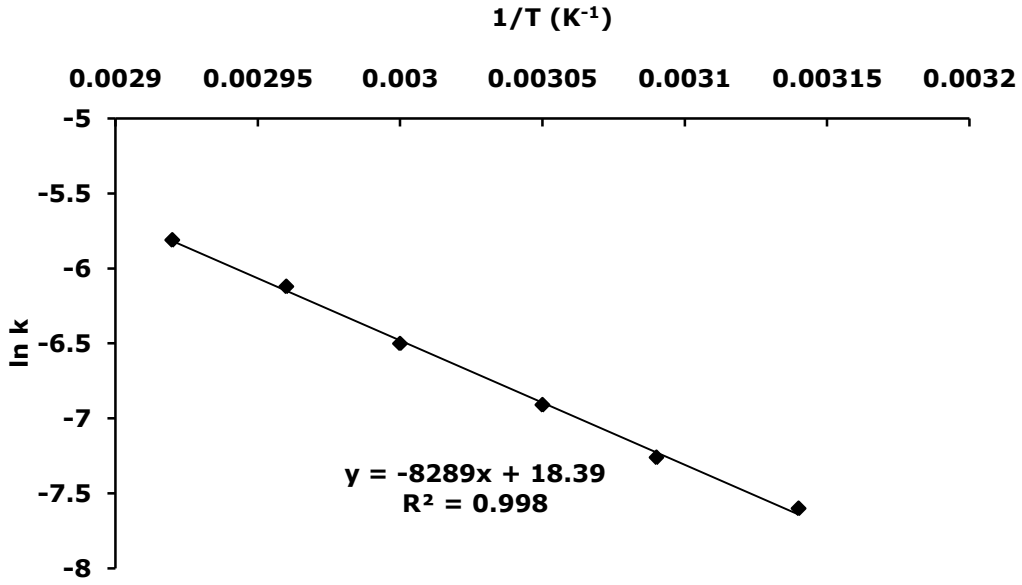

Figure 12. Arrhenius plot correlating lnk with 1/T for the conversion of gmelina oil to biodiesel over KNO_3 activated MgO-ZnO composite**.**

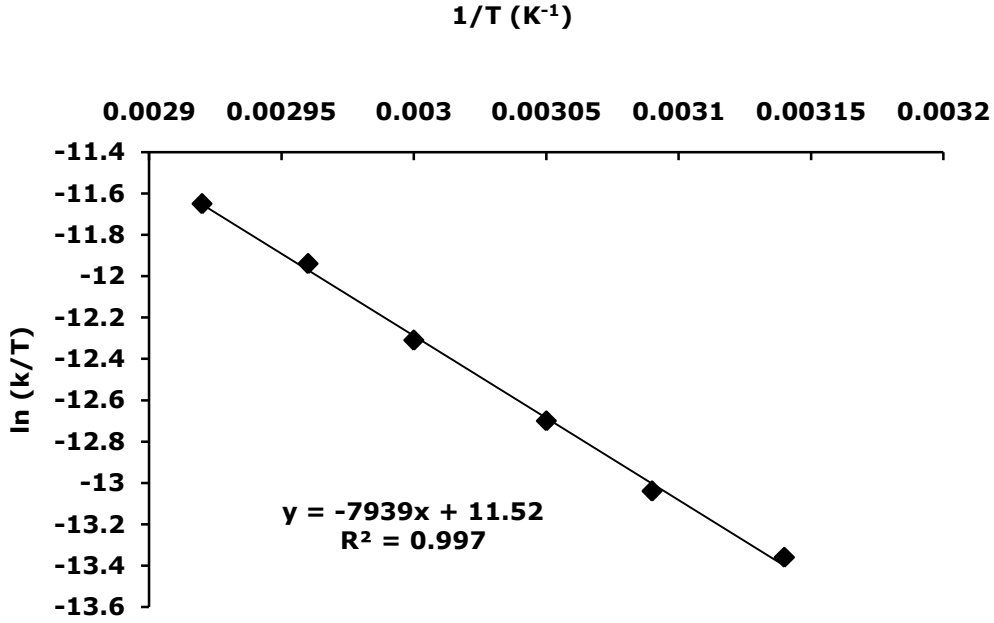

Figure 13. Eyring plot correlating ln(k/T) with 1/T for the conversion of gmelina oil to biodiesel over KNO_3 activated MgO-ZnO composite.

Table 5. Activation energies of gmelina methyl esters and reference values from selected literature.

Methyl esters*	ΔG (kJ/mol)	ΔH (kJ/mol)	ΔS (kJ/mol K)	Reference
GME	100.50	66.004	-0.102	This work
RME	105.6	139.5	-98.0	(34)
CME	96.128	36.124	-180.19	(35)
SPME	92.71	16.35	-232.83	(33)

*Gmelina methyl esters (GME), rapeseed methyl esters (RME), Chlorella methyl esters (CME), *Spirulina platensis* methyl esters (SPME).

The activation properties for gmelina biodiesel are presented in Table 5. Also in the same table for the sake of comparison are thermodynamic properties of the methyl esters of rapeseed, *Chlorella* and *Spirulina platensis*. The Gibbs free energy, enthalpy and entropy of the gmelina methyl esters produced by the heterogeneous catalyst are 100.50 kJ/mol, 66.00 kJ/mol and -0.102 kJ/mol K. The corresponding activation properties of the NaOH base system are 92.14

kJ/mol, 34.23 kJ/mol and -0.174 kJ/mol K. The enthalpies of activation are within the range reported in various literature. As seen from the Table, the gmelina transesterification process is characterized by negative entropies of smaller magnitude which implies the formation or more ordered transient structures en route the formation of methyl esters (36).

CONCLUSIONS

Methyl esters were successfully produced from gmelina oil via methanolysis using NaOH and for the first time compared with KNO_3 activated MgO-ZnO. At optimal reaction condition, the biodiesel yields were significant for both the heterogeneous and homogeneous processes. Petroselinate or 6-octadecanoic acid ester was the major product and its fuel properties are within ASTM limits. It still remains a challenge to achieve a combination of high yield, low methanol-oil molar ratio and short reaction time with heterogeneous catalysts relative to the conventional base process.

ACKNOWLEDGEMENTS

The authors of this paper acknowledge the support of all of the staff of Quality Control Unit, Production, Programming and Quality Control Department, Kaduna Refinery and Petrochemical Company (KRPC), and Nigerian National Petroleum Corporation (NNPC).

REFERENCES

1. Ullah Z, Bustam MA, Man Z. Biodiesel production from waste cooking oil by acidic ionic liquid as a catalyst. Renewable Energy. 2015; 77: 521-6.

2. Sun K, Lu J, Ma L, Han Y, Fu Z, Ding J. A comparative study on the catalytic performance of different zeolites for biodiesel production. Fuel. 2015; 158: 848-54.

3. Feyzi M, Shahbazi Z. Preparation, kinetic and thermodynamic studies of Al–Sr nanocatalysts for biodiesel production. Journal of the Taiwan Institute of Chemical Engineers. 2017; 71: 145-155.

4. Ortiz-Martínez PA, Andreo-Martínez P, García-Martínez N, Pérez de le Ríos, Hernández-Fernández FJ, Quesada-Medina J. Approach to biodiesel production from microalgae under supercritical conditions by the PRISMA method. Fuel Processing Technology. 2019; 191: 211-222.

5. Shahir VK, Jawahar CP, Suresh PR, Vinod V. Experimental Investigation on Performance and Emission Characteristics of a Common Rail Direct InjectionEngine Using Animal Fat Biodiesel Blends. Energy Procedia, 2017; 117: 283-290.

6. Goh BHH, Ong HC, Cheah MY, Chen W-H, Yu KL, Mahlia TMI. Sustainability of direct biodiesel synthesis from microalgae biomass: A critical review. Renewable and sustainable Energy Reviews. 2019; 107: 59-74.

7. Tural S. Zinc perchlorate hexahydrate catalyzed mono- and bis-transesterification of malonic esters. Turkish Journal of Chemistry. 2008; 32: 169-79.

8. Alhassan FH, Rashid U, Taufiq-Yap YH. Biodiesel synthesis catalyzed by transition metal oxide: Ferric-manganese doped tungstated/molybdena nanoparticle catalyst. Journal of Oleo Science.2014; 10: 1-8.

9. Lam MK, Lee KT, Mohamed AR. Homogeneous, heterogeneous and enzymatic catalysis for transesterification of high free fatty acid oil (waste cooking oil) to biodiesel: A review. Biotechnology Advances. 2010; 28: 500-518.

10. Mehra T., process optimization biodiesel production from cedar wood oil (*Cerdrus deodara*) using response surface methodology, SAE Technical paper 2018-01-0665, 2018.

11. Raita M, Laothanachareon T, Champreda V, Laosiripojana N. Biocatalytic esterification of palm oil fatty acids for biodiesel production using glycine-based cross-linked protein coated microcrystalline lipase. Journal of Molecular Catalysis. B: Enzymatic. 2011; 73: 74-9.

12. Ramachandran K, Suganya T, Nagendra GN, Renganathan S. Recent developments for biodiesel production by ultrasonic assisted transesterification using different heterogeneous catalysts: A review. Renewable & Sustainable Energy Reviews. 2013; 22: 410-418.

13. Istadi I, Prasetyo AP, Nugroho TS. Characterization of K_2O/CaO-ZnO catalyst for transesterification of soybean oil to biodiesel. Procedia Environmental Science. 2014; 23: 394-9.

14. Abdulkareem-Alsultan G, Asikin-Mijan N, Lee HV, Taufiq-Yap YH. A new route for the synthesis of La-Ca oxide supported on nano activated carbon via vacuum impregnation method for one pot esterification transesterification reaction. Chemical Engineering Journal. 2016; 304: 61–71.

15. Kesić Ž, Lukić I, Brkić D, Rogan J, Zdujić L, Liu H, Skala D. Mechanochemical preparation and characterization of CaO·ZnO used as catalyst for biodiesel synthesis. Applied Catalysis, A: General. 2012; 427: 58– 65.

16. Kesić Ž, Lukić I, Zdujić L, Liu H, Skala D. Mechanochemical synthesis of $CaO{\cdot}ZnO.K_2CO_3$ catalyst:Characterization and activity for methanolysis of sunflower oil. Chemical Industry and Chemical Engineering Quarterly. 2015; 21(1): 1−12.

17. Fuwape JA, Onyekwelu JC, Adekunle, VAJ. Biomass equations and estimation for *Gmelina arborea* and *Nauclea diderrichii* stands in Akure forest reserve. Biomass & Bioenergy. 2001; 21: 401-5.

18. Kansedo J, Lee KT. Process optimization and kinetic study for biodiesel production from nonedible sea mango (*Cerbera odollam*) oil using response surface methodology. Chemical Engineering Journal. 2013; 214: 157-64.

19. Šánek L, Pecha J, Kolomaznik K, Bařinová M. Biodiesel production from tannery fleshings: Feedstock pretreatment and process modeling. Fuel. 2015; 148: 16-24.

20. Okoro LN, Fadila IS, Mukhtar L, Clifford N. Thermodynamic and viscometric evaluation of biodiesel and blends from olive oil and cashew nut oil. Research Journal of Chemical Sciences. 2011; 1(4): 90-7.

21. AOCS Methods Ca 5a-40, Official methods and recommended practices of the American Oil Chemists' Society. American Oil Chemists Society, Champaign IL, USA; 2000a.

22. AOCS Method Cd 3b-76, Official methods and recommended practices of the American Oil Chemists' Society, 5th Ed., American Oil Chemists Society, Champaign IL, USA; 2000b.

23. ASTM Method D6751-02 "Standard specification for biodiesel fuel (B100) blend stock for distillate fuels" ASTM International, West Conshohocken, PA, Pennsylvania, United States of America; 2002.

24. Das S, Khushalani D. Nonhydrolytic route for synthesis of ZnO and its use as a recyclable photocatalyst. Journal of Physical Chemistry C. 2010; 114: 2544–50.

25. Etacheri V, Roshan R, Kumar V. Mg-doped ZnO nanoparticles for efficient sunlight-driven photocatalysis. ACS Applied Materials & Interfaces. 2012; 4: 2717-25.

26. Feyzi M, Zinatizdeh AAL, Nouri P, Jafari F. Catalytic performance and characterization of promoted K-La/ZSM-5 nanocatalyst for biodiesel production. Iranian Journal of Chemistry and Chemical Engineering. 2018; 37(2): 33-44.

27. Feyzi M, Khajavi G. Investigation of biodiesel production using modified strontium nanocatalysts supported on the ZSM-5 zeolite. Industrial Crops and Products. 2014; 58: 298–304.

28. Meher LC, Naik SN, Das LM. Methanolysis of *Pongamia pinnata* (Karanja) oil for production of biodiesel, Journal of Scientific and Industrial Research. 2004; 63: 913-8.

29. Hoekman SK, Broch A, Robbins C, Ceniceros E, Natarajan M. Review of biodiesel composition, properties, and specifications. Renewable and Sustainable Energy Reviews. 2012; 16: 143– 69.

30. Rashid U, Anwar F, Moser BR, Knothe G. Moringa oleifera oil: A possible source of biodiesel. Bioresource Technology. 2008; 99: 8175–9.

31. Knothe G. "Designer" Biodiesel: Optimizing fatty ester composition to improve fuel properties. Energy Fuels. 2008; 22: 1358–64.

32. Berman P, Nizri S, Wiesman Z. Castor oil biodiesel and its blends as alternative fuel, Biomass & Bioenergy. 2011; 35: 2861-6.

33. Nautiyal P, Subramanian KA, Dastidar MG. Kinetic and thermodynamic studies on biodiesel production from *Spirulina platensis* algae biomass using single stage extraction-transesterifcation process. Fuel. 2014; 135: 228-34.

34. Astria DF, Ilvania CV, Fraderico AL, Heiddy MA, Vitor HM. Thermodynamic analysis of the kinetics reaction of the production of FAME and FAEE using Novazyme-435 as catalyst. Fuel Processing Technololgy. 2011; 92: 1007-11.

35. Ahmad AL, Mat Yasin NH, Derek CJC, Lim JK. Kinetic studies and thermodynamics of oil extraction and transesterification of Chlorella sp. for biodiesel production. Environmental Technology. 2014; 35: 881-7.

36. Engel T, Reid P. Physical chemistry. Pearson Education, San Fransisco; 2006.